The Reducing Effect of Sirolimus on Angiomyolipoma is Determined by Decrease of Its Fat-Poor Compartments and Is Associated with Striking Reduction of Vascular Structures

Elieser Hitoshi Watanabe (elieserhw@yahoo.com)
Universidade de Sao Paulo Faculdade de Medicina https://orcid.org/0000-0002-3371-6019
Fernando Morbeck Almeida Coelho
Universidade de Sao Paulo Faculdade de Medicina
Hilton Leão Filho
Universidade de Sao Paulo Instituto de Radiologia
Bruno Eduardo Pedroso Balbo
Universidade de Sao Paulo Faculdade de Medicina
Precil Diego Neves
Universidade de Sao Paulo Faculdade de Medicina
Fernanda Maria Franzin
Universidade de Sao Paulo Faculdade de Medicina
Fernando Ide Yamauchi
Universidade de Sao Paulo Faculdade de Medicina
Luiz Fernando Onuchic
Universidade de Sao Paulo Faculdade de Medicina

Research

Keywords: Aneurysm, Angiomyolipoma, Hemorrhage, Sirolimus, Tuberous sclerosis

Posted Date: March 17th, 2020

DOI: https://doi.org/10.21203/rs.3.rs-17408/v1

Abstract

Background: Renal angiomyolipomas hemorrhage is strongly associated with their size and vascular constitution. Since previous studies showed that mTOR inhibitors can differentially act in distinct cell lines, we analyzed the effects of sirolimus on the volume of different components of angiomyolipomas in patients with tuberous sclerosis complex, including vascular structures. We retrospectively analyzed 23 angiomyolipomas from 10 patients treated with sirolimus. An approach based on a Hounsfield-unit threshold was used to classify angiomyolipomas in fat-rich, fat-poor and intermediate-fat tumors, and to categorize tumor compartments in fat rich, fat poor, intermediate fat and highly vascularized. Diameter variations were measured to assess the effects on aneurysmatic/ectatic vascular formations.

Results: Volume reduction following treatment with sirolimus was higher in fat-poor than fat-rich angiomyolipomas. Tumor reduction was mainly determined by decrease of the fat-poor and highly-vascularized compartments, with a lesser contribution of the intermediate-fat component, while the volume of the fat-rich compartment increased. Broad liposubstitution was observed in some tumors. Massive reduction of aneurysmatic/ectatic vascular structures was observed, with disappearance of such lesions in most cases.

Conclusions: Our study showed that sirolimus reduces the size of angiomyolipomas by decreasing primarily their highly-vascularized and fat-poor compartments. This effect is associated with a remarkable reduction of tumoral aneurysms/ectatic vessels and other vascular structures. Our findings revealed, therefore, the likely mechanism responsible for the reported risk-decreasing effect of mTOR inhibitors on angiomyolipoma bleeding. Our findings also expand the understanding the biology of this tumor, supporting a role for mTOR in maintenance, and maybe assembling, of blood vessels in angiomyolipomas.

Background

Renal angiomyolipomas (AMLs) are neoplasms originated from the perivascular epithelium, containing adipocyte-like, muscle-like and epithelioid cells as well as dysmorphic blood vessels (1, 2). AMLs affect up to 2.2% of general adult population(3) and are usually sporadic, however approximately 10% of the cases are associated with tuberous sclerosis complex (TSC).(4) TSC is characterized by the development of neoplasm in various organs and tissues, particularly skin, central nervous system, kidneys, lungs and heart (5, 6). Notably, AMLs have been reported in 49–60% of TSC patients evaluated by renal imaging (7, 8). Renal AMLs have also been associated with pulmonary lymphangioleiomyomatosis (LAM) both in the scope of TSC and in sporadic cases (9, 10). Interestingly, LAM affects almost exclusively females, is present in ~ 30% of the TSC patients, and 47–60% of its sporadic cases develop AMLs (11, 12).

Although small AMLs rarely cause relevant complications or symptoms, larger tumors may compress adjacent structures and lead to abdominal discomfort or pain (4, 13, 14). AML-related complications also

include kidney impingement, vena cava and retroperitoneal infiltration, and hemorrhage secondary to aneurysm rupture, a potentially lethal event (4, 14–18).

Sporadic and TSC-associated AMLs share a common molecular pathogenetic mechanism, characterized by loss of suppression of mammalian (mechanistic) target of rapamicyn (mTOR) (19, 20). This signaling pathway promotes protein synthesis, cell hypertrophy and proliferation (19, 21). Its inappropriate hyperactivation, therefore, favors tumor development and growth. Based on this mechanism, clinical trials with mTOR inhibitors (mTORi) were carried out, showing striking reduction of AML size in a safe setting (22–26).

The effects of mTORi on the different AML components, however, are not well characterized. A recent study reported a heterogeneous volume-reducing effect of the mTORi everolimus on AMLs. In that study a more efficient reduction was observed in fat-poor tumors (27), however, the effects on the different tumor compartments have not been assessed. Since hemorrhage is strongly associated with tumor vascularization and presence of intra-tumoral aneurysms larger than 0.5 cm (28, 29), the response of this compartment to mTORis is critical to understand the role of mTOR in AML vascular structure. Moreover, given that bleeding is the most relevant clinical aspect associated with AMLs, it is essential to evaluate the effect of these drugs on the patient's bleeding risk. In this study we unraveled different effects of sirolimus on the distinct AML compartments as well as its remarkable reduction effect on the vascular tumor component.

Materials And Methods

Study Population and Radiologic Analyses

We retrospectively identified nine patients followed at the University of São Paulo Medical Center between April/2010 and March/2018 treated with sirolimus for at least three months due to large AMLs. All patients were submitted to computed tomography scan (CT) prior and after the mentioned period of sirolimus therapy and had pre- and post-contrast imaging.

In non-contrasted sequences we classified the lesions in three categories based on the average tumor attenuation, expressed in Hounsfield units (HU): fat-rich (<-30 HU; FRT), intermediate-fat (≥-30 and ≤ 30 HU; IFT) and fat-poor (> 30 HU; FPT). All patients were screened for FRT, IFT and FPT, having one representative lesion of each profile been selected for analysis whenever identified. Total volume response to sirolimus was quantified for all included tumors. This evaluation was followed by corticomedullary-phase analysis, which allowed the measurement of such a response in specific AML compartments.

The pixel distribution associated with each tumor was initially plotted according to their attenuation pattern, giving rise a specific histogram (Figure S1). Pixel densities below − 30 HU corresponded to fat-rich compartments (FRC), densities ≥-30 and < 30 HU were associated with intermediate-fat compartments (IFC), attenuation ≥ 30 and < 100 HU indicated a fat-poor compartment (FPC), and pixel

densities ≥ 100 HU identified highly-vascularized compartments (HVC). This approach allowed the quantification of volume response to sirolimus for each of the AML compartments, characterizing its potentially differential effects upon each of the tumor components. To improve the assessment of sirolimus actions on the AML vascular structures, each of the analyzed tumors had the diameter of its largest aneurysmatic/ectatic vessel determined following the CT corticomedullary-phase.

Statistical Analyses

Data on continuous variables were tested for normality using the Shapiro-Wilk test. Since this analysis revealed non-parametric distributions, these data are presented as median and 25 and 75 percentiles. Categorical data are expressed as absolute values and percentages. Non-parametric data were compared using the Mann-Whitney U test for two independent samples or the Wilcoxon test for two-time measures. Non-parametric data associated with multiple groups were compared using the Kruskal-Wallis test, while multiple comparisons were corrected applying the Bonferroni method.

Given the limited number of cases, multivariable analyses for binary endpoints were performed using logistic regression with Firth´s penalization (30). Statistical significance was considered for asymptotic $P < 0.05$. The analyses were performed using SPSS 24.0, GraphPad Prism 8.0 and Stata 16.0.

Results

Baseline Patient and Angiomyolipoma Features

We selected 10 patients that fulfilled all inclusion criteria. Twenty-three AMLs from these patients were selected for analyses, since in seven cases one of the AML fat profiles was not identified. The mean AML pre-treatment size was 4.5 cm (2.3–5.1). The baseline features of analyzed patients and respective tumors are depicted in Table 1.

Table 1
Characterization of patients and angiomyolipomas

	N	Median (Percentiles 25–75%)
Patient age	10	34.8 (22.9–51.6)
Sirolimus serum level (ng/mL)	7	8.1(7.6–9.6)
Time of treatment before CT (days)	23	258.0 (199.0-332.0)
Pre-treatment tumor size (mm)	23	40.0 (23.0–51.0)
Pre-treatment aneurysm diameter (mm)	17	2.0 (1.0-4.5)
FRT pre-treatment total volume (cm^3)	7	4.8 (2.4–23.4)
FRT pre-treatment size (mm)	7	25.0 (19.0–40.0)
IFT pre-treatment total volume (cm^3)	6	15.7 (2.4-260.7)
IFT pre-treatment size (mm)	6	40 (16.25–93.7)
FPT pre-treatment total volume (cm^3)	10	35.9 (20.0-167.8)
FPT pre-treatment size (mm)	10	45.0 (35.8–78.0)
CT: computed tomography; FPT: fat-poor tumor; FRT: fat-rich tumor, FP; IFT: intermediate-fat tumor.		

Sirolimus Reduces Tumor Volume More Effectively in Fat-Poor AMLs

As expected, sirolimus effectively reduced tumor volume, leading to a median AML volume reduction of -52.3% (-68.7- -12.2) (Fig. 1). The tumoral volume response, however, was heterogeneous among the different tumor fat profiles. FRTs presented milder responses to sirolimus than FPT [-12.2% (-27.1-38.6) versus − 65.5% (-74.3- -61.1), P = 0.014] (Fig. 2). IFTs, in turn, displayed a volume decrease of -45.2% (-58.0- 6.2), a value not significantly different from the FRT and FPT groups (Fig. 1).

AML Fat Poorness Predicts a Better Response to Sirolimus

Using the Firth's logistic regression for an at-least-50% response of volume reduction, we evaluated fat profile, gender, age, serum sirolimus level, treatment length and tumor size at baseline as potential predictors of volume response to sirolimus. This analysis identified the FPT pattern as the sole predictor of an at-least-50% decrease in tumor volume following this treatment (Table 2).

Table 2

Firth's logistic regression for an at-least-50% tumor volume reduction

Variable	Odds Ratio	P	95% CI
AML fat profile FRT IFT FPT	1 12.9 129.8	0.210 0.017	0.3–197.0 2.4-7039.3
Gender	1.1	0.975	0.0-52.6
Age	1.1	0.446	0.9–1.2
Sirolimus serum level	0.9	0.879	0.4–2.3
Treatment length	1.0	0.318	0.9-1.0
Tumor size at baseline	1.0	0.560	0.9-1.0
CI: confidence interval; FPT: fat poor tumor; FRT: fat rich tumor; IFT: intermediated fat tumor.			

Sirolimus Induces Massive Reduction of AML Vascular Structures and Is Essentially Not Effective in the Fat-Rich Compartment

Volume analyses of the different AML compartments following sirolimus revealed that all components, except for FRC, responded to treatment with significant volume reduction (Fig. 3a and 4). Notably, HVC presented a remarkable volume decrease following this therapy [0.9 cm^3 (0.1–33.2) versus 0.10 cm^3 (0.0-2.3), P = 0.002] (Fig. 3b), an effect that represented a 90.0% (80.7–98.5) volume reduction among the evaluated AMLs (Fig. 3a). The variations in ectatic vessel/aneurysm size were consistent with this finding, revealing disappearance or massive reduction in most of the assessed vascular lesions [2.0 cm (1.0-4.5) versus 0.0 cm (0.0–1.0), P < 0.001] (Fig. 3b, 3c and 5).

As expected based on the robust response of fat-poor AMLs to sirolimus, FPC presented massive volume reduction following this treatment [2.5 cm^3 (0.3–19.0) to 0.5 cm^3 (0.1–8.6), P = 0.002] (Fig. 3d), a response of 77.8% (25.0-91.9) volume decrease among the tumors (Fig. 3a). The AML compartment with attenuation of 30 HU or more was, in fact, responsible for 76.7% (25.6–100.0) of total tumor reduction.

Surprisingly, FRC volume not only did not decrease in response to sirolimus but also substantially increased in most cases. FRC volume, in fact, grew from 1.4 cm^3 (0.25–7.8) to 2.6 cm^3 (0.5–18.2) following this treatment, P = 0.012 (Fig. 3e), an effect reflected in a 105.9% growth (21.7-256.6) (Fig. 3a).

Consistently with the aforementioned findings, IFC volume responded to treatment with sirolimus with an intermediate behavior between FRC and FPC. Indeed, the IFC volume decreased from 2.5 cm^3 (0.8–10.0)

to 1.5 cm^3 (0.3–4.9) after the mentioned therapy, P = 0.014 (Fig. 3f), a response also expressed as 61.5% (-11.7-75.0) volume reduction among the analyzed AMLs (Fig. 3a). It must be noted, however, that the IFC volume change was significantly different from the FRC one but did not significantly differ from the FPC volume variation (Fig. 3a).

As a result of these differential effects of sirolimus on the AML compartments, this treatment leads to critical tumor structural changes. Within the scope of visible transformations of the tumor fat profile, some FPTs respond to sirolimus becoming FRTs (Fig. 6).

Discussion

Renal complications constitute the main cause of death among TSC patients (31–33). A significant portion of such complications include AML hemorrhage. Although end-stage renal disease is reported at low rates in TSC patients (34, 35), the studied populations are usually young. Notably, up to 40% of the TSC patients develop chronic kidney disease (CKD), exhibiting an estimated glomerular filtration rate equivalent to 30-year-older subjects from the general population (36). While the pathogenesis of TSC-associated CKD remains not completely understood, several factors are known to contribute to renal function decline, including tumor bleeding, tumor encroaching to normal surrounding renal tissue, renal cystic involvement, focal and segmental glomerulosclerosis and tubulointerstitial disease. A molecular mechanism involving TSC1 or TSC2 loss of function in renal parenchyma has also been proposed to play a role in reducing glomerular filtration rate (2, 37). Invasive interventions to prevent tumor hemorrhage, moreover, including partial nephrectomy and selective arterial embolization, can also impact on early loss of renal function as a consequence of loss of functional renal tissue (32). It should be noted that these invasive procedures are not uncommon in clinical practice (32, 36), given the potential lethality associated with AML hemorrhage. A recent databank study reported that 24.2% of TSC patients had at least one invasive kidney intervention.(38) Because TSC patients usually present multiple AMLs, and the incidence increases with age, such interventions usually cannot treat all lesions. Invasive procedures, therefore, are often repeated along life, leading to increased risk of CKD (32).

In response to this scenario, clinical studies have shown efficacy of mTORi in reducing AML volume, supporting these drugs as first-line therapy of asymptomatic AMLs larger than 3 cm in TSC patients (37). Such studies, however, had the primary end-point focused on tumor size reduction, not addressing whether the verified AML shrinkage lowers the bleeding rate and preserves renal function. Interestingly, however, no event of AML bleeding was reported in the extension of the phase 3 study “Everolimus for renal angiomyolipoma in patients with tuberous sclerosis complex or sporadic lymphangioleiomyomatosis (EXIST-2)” (39), a trial that followed 112 patients treated with everolimus for a median period of 28.9 weeks. This finding suggests a bleeding protective role of mTORi.

Despite the recognition of this effect of mTORi on AML volume, the response to these drugs has been shown to significantly vary among such tumors (39). In addition, AMLs are neoplasms histologically complex, with components derived from at least three distinct cellular phenotypes. Based on these two

observations, we raised the hypothesis that mTORis might have different effects on distinct tumor components and compartments, and investigated this possibility in AMLs with different constitutions from a series of TSC patients. Of note, the elucidation of this effect might not only clarify a complex biological problem but also bring novel, important information to the clinical scenario. Clinical benefits could potentially include the development of predictors for AML response to mTORi as well as risk modifications associated with disease complications.

As expected, AMLs responded to sirolimus with volume reduction, a response that significantly varied among the tumors. Interestingly, our CT analyses revealed differential effects of sirolimus on AMLs with distinct proportions of fat. Fat-poor AMLs displayed a dramatic volume reduction response to sirolimus while such an effect was much milder in fat-rich tumors. In consistency with these findings, intermediate-fat AMLs presented an intermediate volume decrease behavior between fat-poor and fat-rich tumors. An important clinical derivative of this analysis was the finding that in AMLs fat poorness predicts a more effective response to sirolimus.

Our findings also revealed that the differential effect of sirolimus on AMLs is essentially based on differential effects on specific tumor compartments. Our data showed a primary reduction of the fat-poor portions of the tumors. Interestingly, the profound effect of sirolimus on the FPCs and HVCs promoted the transformation of some FPTs into FRTs, a finding not yet reported. The liposubstitution observed in such AMLs represents, in fact, the most striking translation of the remarkable differential actions of mTORi in the different AML compartments. Our findings also unraveled a dramatic decrease of vascular aneurysmatic formations. In line with this concept, the volume of the AML fat-rich compartment did not decrease, but instead increased, in response to treatment. Our findings of massive reduction of the vascular tumor components in response to sirolimus, in turn, suggest that this treatment is likely protective against AML bleeding.

Our data are in line with previous observations that in vitro effects of sirolimus differ among distinct cell lineages (40) and TSC patients display high levels of the pro-angiogenic molecules VEGF-A and VEGF-D (vascular epithelial growth factors A and D) (41). mTOR inhibitors, therefore, could differentially act in the different components of AML, with particularly high efficiency on vascular formations. mTOR complex 1 (mTORC1), in fact, is known to drive HIF-1α (hypoxia-induced factor 1α) and VEGF-A signaling via multiple mechanisms involving 4E-BP1 (eukaryotic translation initiation factor 4E-binding protein 1), S6K1 (p70 ribosomal protein S6 kinase 1) and STAT3 (signal transducer and activator of transcription 3), an angiogenic process potentially attenuated by sirolimus (42). Interestingly, this mechanism is associated with acceleration of endothelial senescence (43). It is possible, therefore, that the molecular basis of the differential mTORi effects on the AML compartments is based on VEGF downregulation induced by sirolimus through inhibition of mTORC1 (44). Reduction of VEGF-D circulating levels was also reported in patients receiving rapamicyn.(24) The remarkable reduction of AML vascular components shown in our study suggests that mTOR activity is fundamental to the maintenance of such structures in AMLs. Moreover, since aneurysms are the main determinant for tumor hemorrhage(28), the inhibition of maintenance and development of aneurysmatic/ectatic formations induced by mTORi is the likely

mechanism responsible for the reduction of bleeding occurrence observed in the EXIST-2 study and its extension (22, 39).

Conclusions

Our findings suggest, therefore, that image analysis of AML compartments is likely helpful to predict tumor response to mTORi. Our data revealed, moreover, that treatment with sirolimus not only reduces the tumor size but selectively acts on components associated with more often and more severe clinical complications, such as AML bleeding. Our results provide additional support to the recent recommendation of chronic treatment with mTORi of TSC individuals with AMLs > 3 cm, and suggest that the presence of large aneurysms/vascular formations should be an independent criterium to initiate this therapy.

Abbreviations

AML: angiomyolipoma; CKD: chronic kidney disease; CT: computer tomography scan; FPC: fat-poor compartiments; FRC: fat-rich compartiments; FPT: fat-poor tumor; FRT: fat-rich tumor; HIF-1α: hypoxia-induced factor 1α; HU: Hounsfield unit; HVC: high vascularized compartiments; IFC: intermediate fat compartiments; IFT: intermediate fat tumor; LAM: lymphangioleiomyomatosis; mTOR: mammalian (mechanistic) target of rapamycin; mTORC1: mammalian (mechanistic) target of rapamycin complex 1; mTORi: mammalian (mechanistic) target of rapamycin inhibitor; S6K1: p70 ribossomal protein S6 kinase 1; STAT3: signal transducer and activator of transcription 3; TSC: tuberous sclerosis complex; VEGF-A: vascular epithelial growth factor A; VEGF-D: vascular epithelial growth factor D; 4E-BP1: eukaryotic translation initiation factor 4E-binding protein 1

Declarations

Ethics approval and consent to participate:

This work was approved by HC-FMUSP Research Ethics Committee under CAAE number: 44709915.1.0000.0068

Consent for publication:

Not applicable

Availability of data and materials:

The datasets generated and/or analysed during the current study are not publicly available due to including files and images with personal information of patients, but, are available from the corresponding author on reasonable request.

Competing interests:

All the authors have no conflicts of interest to disclosure.

Funding:

This work was funded by institutional resources from the University of São Paulo Medical Center.

Author´s contributions:

Elieser H Watanabe had a lead role in conceptualization, methodology, formal analysis, investigation, and writing/editing the original draft and had a lead role in data curation, project administration and statistical analysis. Fernando M A Coelho had a supporting role in conceptualization, methodology, writing/editing the original draft, and had a lead role imaging analysis. Hilton Leão Filho had a supporting role in imaging analysis. Bruno E P Balbo had a supporting role in data curation. Precil D M M Neves had a supporting role in data curation. Fernanda M Franzin had a supporting role in data curation and writing/editing the original draft. Fernando I Yamauchi a supportive role in conceptualization, imaging analyses and writing/editing the original draft. Luiz F Onuchic had a lead role in conceptualization, methodology, formal analysis, investigation, and writing/editing the original draft.

Acknowledgements:

We thank the University of São Paulo Medical Center for the support to this study.

References

1. Lienert AR, Nicol D. Renal angiomyolipoma. BJU international. 2012;110(S4):25-7.
2. Dixon BP, Hulbert JC, Bissler JJ. Tuberous sclerosis complex renal disease. Nephron Exp Nephrol. 2011;118(1):e15-20.
3. Rule AD, Sasiwimonphan K, Lieske JC, Keddis MT, Torres VE, Vrtiska TJ. Characteristics of renal cystic and solid lesions based on contrast-enhanced computed tomography of potential kidney donors. American Journal of Kidney Diseases. 2012;59(5):611-8.
4. Bissler JJ, Kingswood JC. Renal angiomyolipomata. Kidney international. 2004;66(3):924-34.
5. Samueli S, Abraham K, Dressler A, Groeppel G, Jonak C, Muehlebner A, et al. Tuberous Sclerosis Complex: new criteria for diagnostic work-up and management. Wiener klinische Wochenschrift. 2015:1-12.
6. Leung AK, Robson WL. Tuberous sclerosis complex: a review. J Pediatr Health Care. 2007;21(2):108-14.
7. Rakowski SK, Winterkorn EB, Paul E, Steele DJ, Halpern EF, Thiele EA. Renal manifestations of tuberous sclerosis complex: Incidence, prognosis, and predictive factors. Kidney Int. 2006;70(10):1777-82.
8. Casper KA, Donnelly LF, Chen B, Bissler JJ. Tuberous Sclerosis Complex: Renal Imaging Findings 1. Radiology. 2002;225(2):451-6.

9. McCormack FX. Lymphangioleiomyomatosis: a clinical update. CHEST Journal. 2008;133(2):507-16.
10. Avila NA, Dwyer AJ, Rabel A, Moss J. Sporadic lymphangioleiomyomatosis and tuberous sclerosis complex with lymphangioleiomyomatosis: comparison of CT features. Radiology. 2007;242(1):277-85.
11. Chu SC, Horiba K, Usuki J, Avila NA, Chen CC, Travis WD, et al. Comprehensive evaluation of 35 patients with lymphangioleiomyomatosis. CHEST Journal. 1999;115(4):1041-52.
12. Bernstein SM, Newell Jr JD, Adamczyk D, Mortenson RL, King Jr TE, Lynch DA. How common are renal angiomyolipomas in patients with pulmonary lymphangiomyomatosis? American journal of respiratory and critical care medicine. 1995;152(6):2138-43.
13. Dickinson M, Ruckle H, Beaghler M, Hadley H. Renal angiomyolipoma: optimal treatment based on size and symptoms. Clinical nephrology. 1998;49(5):281-6.
14. Harabayashi T, Shinohara N, Katano H, Nonomura K, Shimizu T, Koyanagi T. Management of renal angiomyolipomas associated with tuberous sclerosis complex. J Urol. 2004;171(1):102-5.
15. Kutcher R, Rosenblatt R, Mitsudo S, Goldman M, Kogan S. Renal angiomyolipoma with sonographic demonstration of extension into the inferior vena cava. Radiology. 1982;143(3):755-6.
16. Camunez F, Lafuente J, Robledo R, Echenagusia A, Perez M, Simo G, et al. CT demonstration of extension of renal angiomyolipoma into the inferior vena cava in a patient with tuberous sclerosis. Urologic radiology. 1988;9(1):152-4.
17. Fegan JE, Shah HR, Mukunyadzi P, Schutz MJ. Extrarenal retroperitoneal angiomyolipoma. Southern medical journal. 1997;90(1):59-62.
18. Steiner MS, Goldman SM, Fishman EK, Marshall FF. The natural history of renal angiomyolipoma. J Urol. 1993;150(6):1782-6.
19. Kenerson H, Folpe AL, Takayama TK, Yeung RS. Activation of the mTOR pathway in sporadic angiomyolipomas and other perivascular epithelioid cell neoplasms. Human pathology. 2007;38(9):1361-71.
20. El-Hashemite N, Zhang H, Henske EP, Kwiatkowski DJ. Mutation in TSC2 and activation of mammalian target of rapamycin signalling pathway in renal angiomyolipoma. Lancet. 2003;361(9366):1348-9.
21. Inoki K, Corradetti MN, Guan KL. Dysregulation of the TSC-mTOR pathway in human disease. Nat Genet. 2005;37(1):19-24.
22. Bissler JJ, Kingswood JC, Radzikowska E, Zonnenberg BA, Frost M, Belousova E, et al. Everolimus for angiomyolipoma associated with tuberous sclerosis complex or sporadic lymphangioleiomyomatosis (EXIST-2): a multicentre, randomised, double-blind, placebo-controlled trial. Lancet. 2013;381(9869):817-24.
23. Bissler JJ, McCormack FX, Young LR, Elwing JM, Chuck G, Leonard JM, et al. Sirolimus for angiomyolipoma in tuberous sclerosis complex or lymphangioleiomyomatosis. New England Journal of Medicine. 2008;358(2):140-51.

24. Dabora SL, Franz DN, Ashwal S, Sagalowsky A, DiMario FJ, Miles D, et al. Multicenter phase 2 trial of sirolimus for tuberous sclerosis: kidney angiomyolipomas and other tumors regress and VEGF- D levels decrease. PLoS One. 2011;6(9):e23379.
25. Cabrera López C, Martí T, Catalá V, Torres F, Mateu S, Ballarín Castán J, et al. Effects of rapamycin on angiomyolipomas in patients with tuberous sclerosis. Nefrologia. 2011;31(3):292-8.
26. Davies DM, de Vries PJ, Johnson SR, McCartney DL, Cox JA, Serra AL, et al. Sirolimus therapy for angiomyolipoma in tuberous sclerosis and sporadic lymphangioleiomyomatosis: a phase 2 trial. Clin Cancer Res. 2011;17(12):4071-81.
27. Hatano T, Atsuta M, Inaba H, Endo K, Egawa S. Effect of everolimus treatment for renal angiomyolipoma associated with tuberous sclerosis complex: an evaluation based on tumor density. Int J Clin Oncol. 2018;23(3):547-52.
28. Yamakado K, Tanaka N, Nakagawa T, Kobayashi S, Yanagawa M, Takeda K. Renal Angiomyolipoma: Relationships between Tumor Size, Aneurysm Formation, and Rupture 1. Radiology. 2002;225(1):78-82.
29. Rimon U, Duvdevani M, Garniek A, Golan G, Bensaid P, Ramon J, et al. Large renal angiomyolipomas: digital subtraction angiographic grading and presentation with bleeding. Clin Radiol. 2006;61(6):520-6.
30. Wang X. Firth logistic regression for rare variant association tests. Front Genet. 2014;5:187.
31. Shepherd CW, GOMEZ MR, Lie J, CROWSON CS, editors. Causes of death in patients with tuberous sclerosis. Mayo Clinic Proceedings; 1991: Elsevier.
32. Eijkemans MJ, van der Wal W, Reijnders LJ, Roes KC, van Waalwijk van Doorn-Khosrovani SB, Pelletier C, et al. Long-term Follow-up Assessing Renal Angiomyolipoma Treatment Patterns, Morbidity, and Mortality: An Observational Study in Tuberous Sclerosis Complex Patients in the Netherlands. Am J Kidney Dis. 2015;66(4):638-45.
33. Amin S, Lux A, Calder N, Laugharne M, Osborne J, O'callaghan F. Causes of mortality in individuals with tuberous sclerosis complex. Dev Med Child Neurol. 2017;59(6):612-7.
34. Clarke A, Hancock E, Kingswood C, Osborne JP. End-stage renal failure in adults with the tuberous sclerosis complex. Nephrol Dial Transplant. 1999;14(4):988-91.
35. Vekeman F, Magestro M, Karner P, Duh MS, Nichols T, van Waalwijk van Doorn-Khosrovani SB, et al. Kidney involvement in tuberous sclerosis complex: the impact on healthcare resource use and costs. J Med Econ. 2015;18(12):1060-70.
36. Kingswood JC, Bruzzi P, Curatolo P, de Vries PJ, Fladrowski C, Hertzberg C, et al. TOSCA - first international registry to address knowledge gaps in the natural history and management of tuberous sclerosis complex. Orphanet J Rare Dis. 2014;9:182.
37. Kingswood JC, Bissler JJ, Budde K, Hulbert J, Guay-Woodford L, Sampson JR, et al. Review of the Tuberous Sclerosis Renal Guidelines from the 2012 Consensus Conference: Current Data and Future Study. Nephron. 2016;133(4).

38. Bissler J, Cappell K, Charles H, Song X, Liu Z, Prestifilippo J, et al. Rates of interventional procedures in patients with tuberous sclerosis complex-related renal angiomyolipoma. Curr Med Res Opin. 2015;31(8):1501-7.
39. Bissler JJ, Kingswood JC, Radzikowska E, Zonnenberg BA, Frost M, Belousova E, et al. Everolimus for renal angiomyolipoma in patients with tuberous sclerosis complex or sporadic lymphangioleiomyomatosis: extension of a randomized controlled trial. Nephrol Dial Transplant. 2016;31(1):111-9.
40. Sarbassov DD, Ali SM, Sengupta S, Sheen JH, Hsu PP, Bagley AF, et al. Prolonged rapamycin treatment inhibits mTORC2 assembly and Akt/PKB. Mol Cell. 2006;22(2):159-68.
41. Siroky BJ, Yin H, Dixon BP, Reichert RJ, Hellmann AR, Ramkumar T, et al. Evidence for pericyte origin of TSC-associated renal angiomyolipomas and implications for angiotensin receptor inhibition therapy. Am J Physiol Renal Physiol. 2014;307(5):F560-70.
42. Dodd KM, Yang J, Shen MH, Sampson JR, Tee AR. mTORC1 drives HIF-1α and VEGF-A signalling via multiple mechanisms involving 4E-BP1, S6K1 and STAT3. Oncogene. 2015;34(17):2239-50.
43. Ota H, Eto M, Ako J, Ogawa S, Iijima K, Akishita M, et al. Sirolimus and everolimus induce endothelial cellular senescence via sirtuin 1 down-regulation: therapeutic implication of cilostazol after drug-eluting stent implantation. Journal of the American College of Cardiology. 2009;53(24):2298-305.
44. Guba M, Von Breitenbuch P, Steinbauer M, Koehl G, Flegel S, Hornung M, et al. Rapamycin inhibits primary and metastatic tumor growth by antiangiogenesis: involvement of vascular endothelial growth factor. Nature medicine. 2002;8(2):128-35.

Supplemental Figure

Figure S1: Image-based assessment of sirolimus effects on AMLs. (a-h) Histogram analysis of the AML displayed in Figure 2 shows pixel densities below -30 HU (fat-rich compartments) in a (pre-treatment) and e (post-treatment), ≥-30 and <30 HU (intermediate-fat compartments) in b (pre-treatment) and f (post-treatment), ≥30 and <100 HU (fat-poor compartments) in c (pre-treatment) and g (post-treatment), and ≥100 HU (highly-vascularized compartments) in d (pre-treatment) and h (post-treatment).

Figures

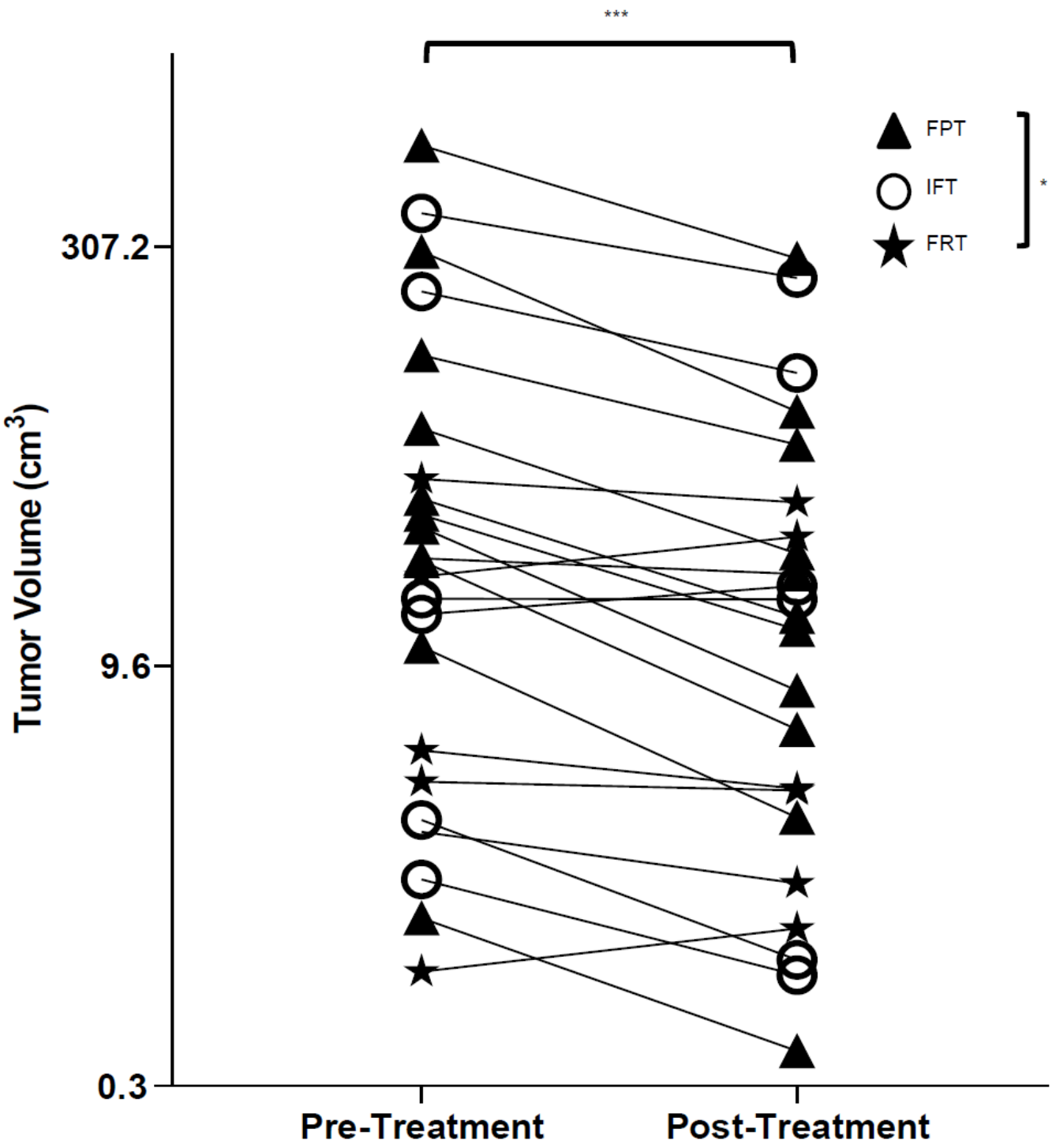

Figure 1

Total tumor volume pre- and post-treatment with sirolimus. Repeated measures were analyzed using the Wilcoxon test, whereas comparisons among tumor fat profiles were performed with the Kruskal-Wallis test. FPT: fat-poor tumor; FRT: fat-rich tumor; IFT: intermediate-fat tumor. * P<0.05, *** P<0.001.

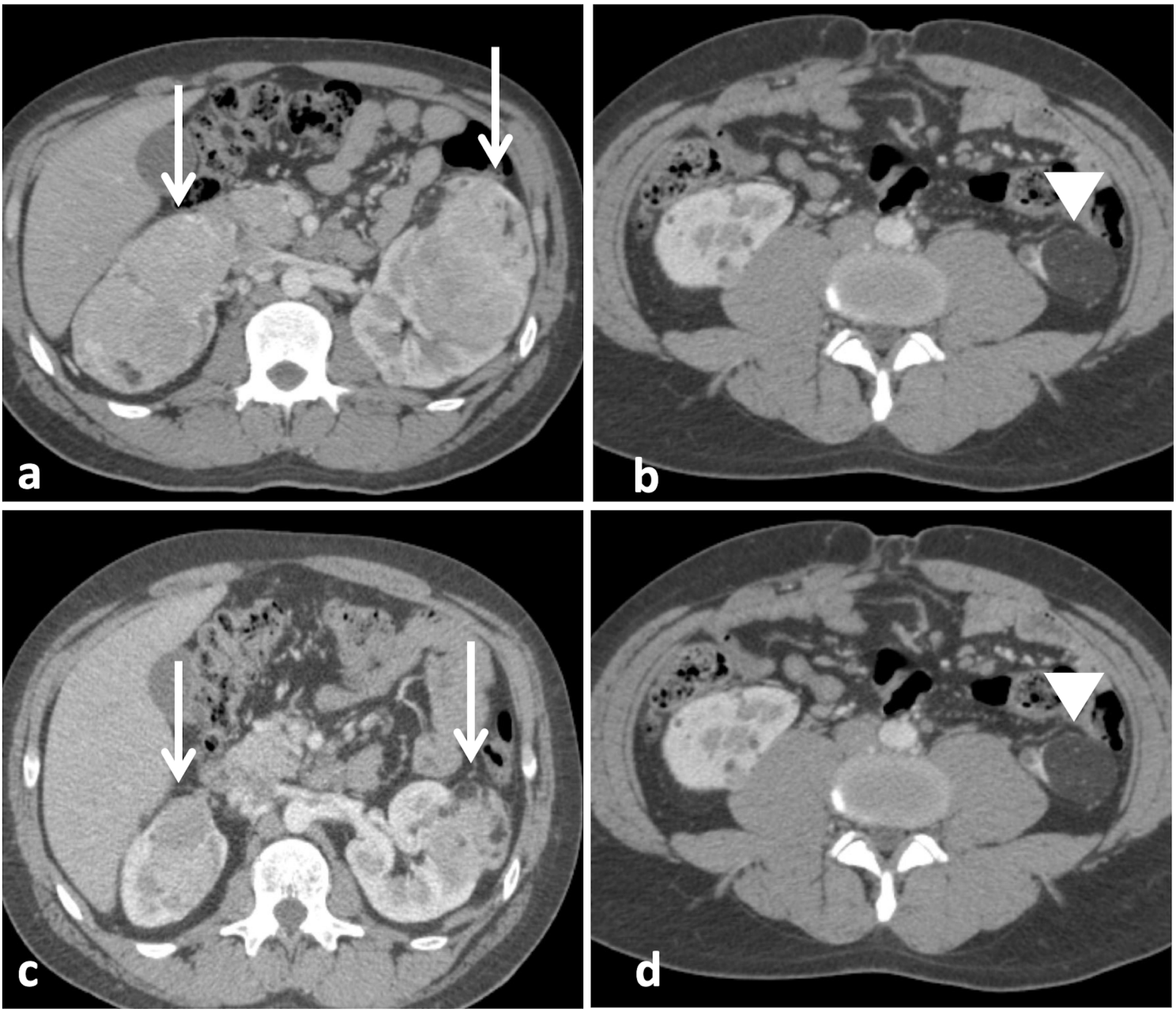

Figure 2

Response of renal AMLs to treatment with sirolimus. (a,b) Axial corticomedullary-phase CT images obtained before treatment show lobulated fat-poor AMLs in both kidneys (arrows) and a fat-rich AML arising from the lower pole of the left kidney (arrowhead). (c,d) Axial corticomedullary-phase CT images acquired after 7 months of treatment show significant volumetric reduction of the fat-poor AMLs (arrows) and nonsignificant change in the fat-rich AML (arrowhead).

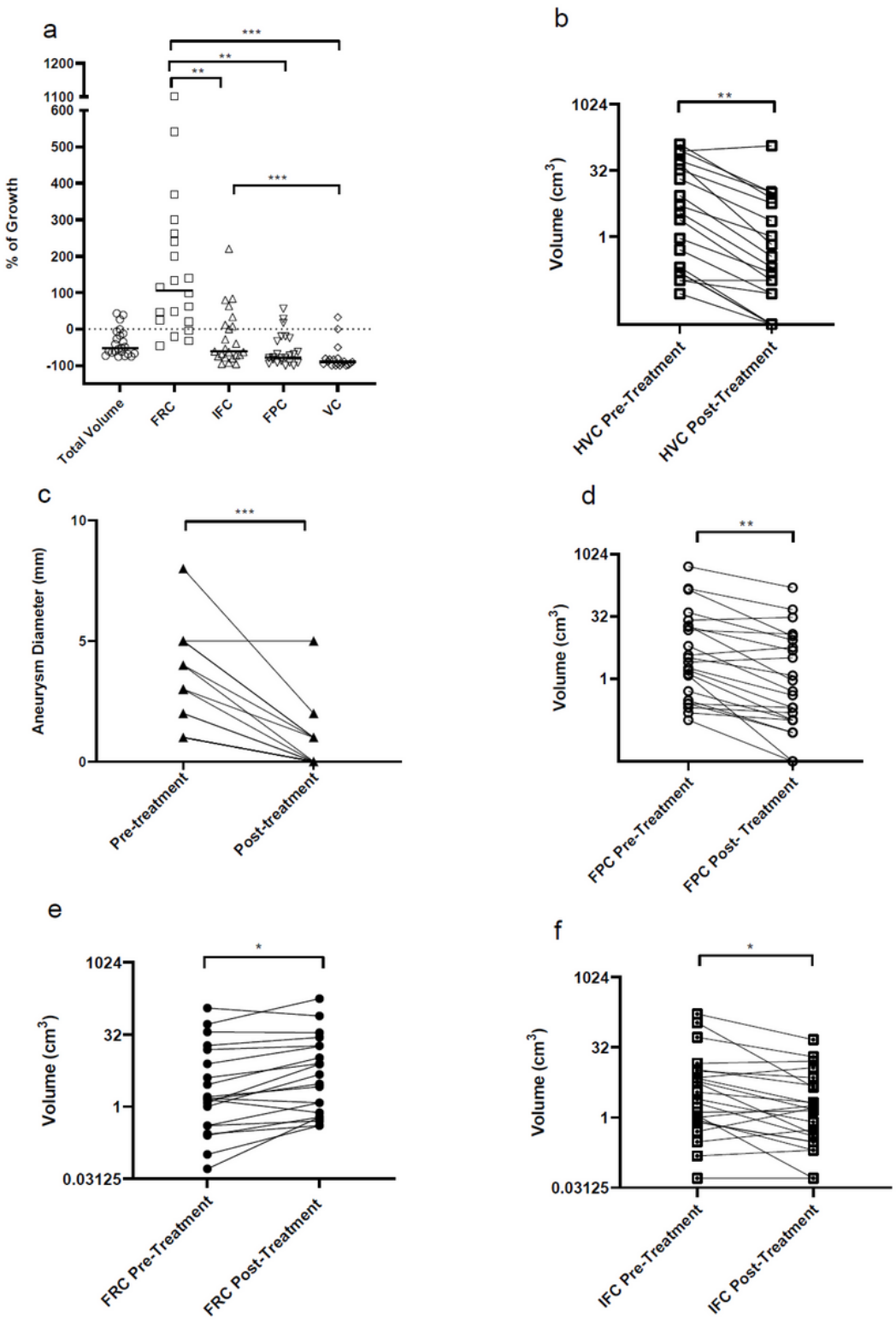

Figure 3

Percent variation of total tumor volume and tumor compartments volume following treatment with sirolimus (a). Variation of tumor compartment volume - HVC (b), FPC (c), FRC (d) and IFC (e) - following treatment with sirolimus - and size variation of angiomyolipoma ectatic vessels/aneurysms (f) in response to sirolimus. HVC, FPC and IFC presented significant volume reduction while FRC displayed volume increase. Comparisons between different groups were performed with Kruskal-Wallis test and

repeated measures were analysed with the Wilcoxon test. FPC: fat-poor compartment; FRC: fat-rich compartment; HVC: highly-vascularized compartment; IFC: intermediate-fat compartment. * P<0.05, ** P<0.01, *** P<0.001.

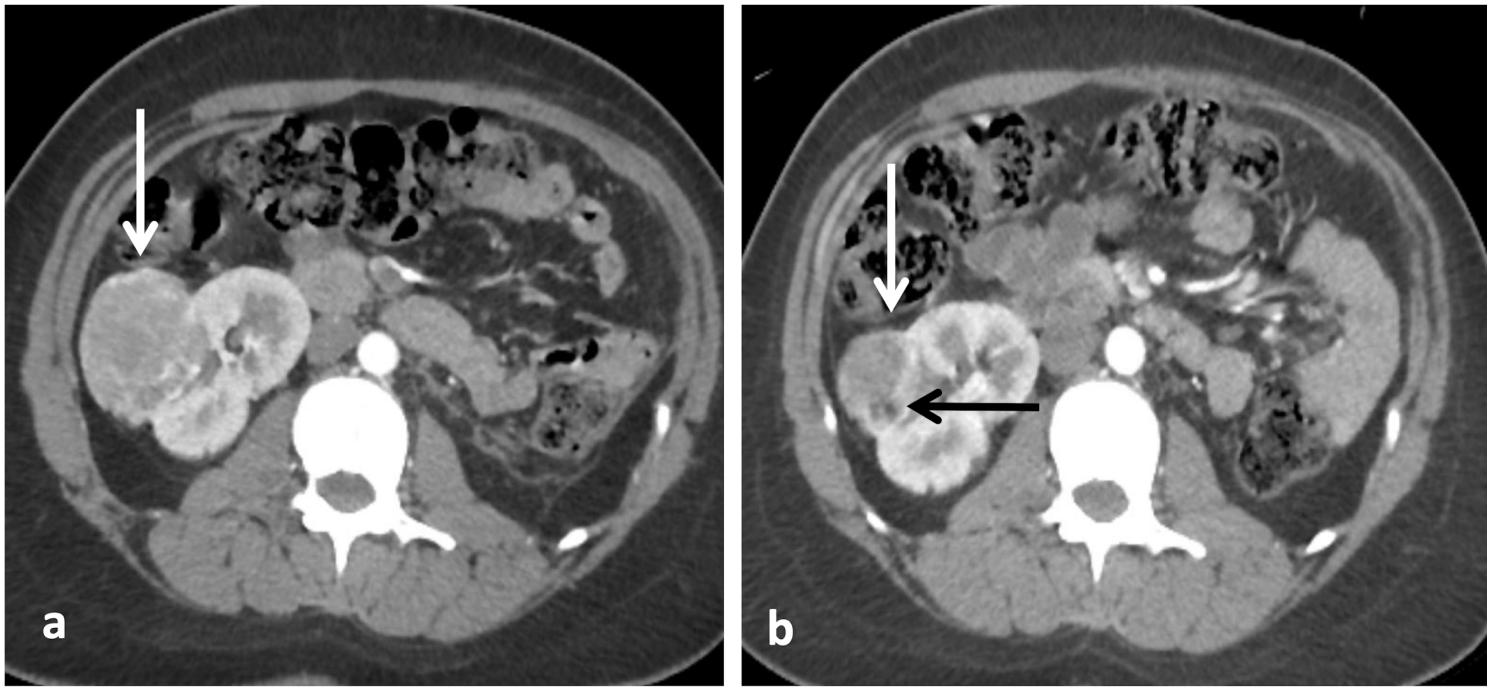

Figure 4

Change in AML volume and fat-containing pattern in response to sirolimus. (a) Pre-treatment axial corticomedullary-phase CT scan shows a right renal fat-poor AML (white arrow). (b) Post-treatment axial corticomedullary-phase CT image reveals tumor volume reduction (white arrow) while the fat component becomes visible (black arrow). Note that the AML total volume reduction (from 76.4 cm^3 to 26.9 cm^3) occurred due to diminishment of the fat-poor (from 60.1 cm^3 to 13.0 cm^3) and highly-vascularized (from 15.4 cm^3 to 11.3 cm^3) compartments.

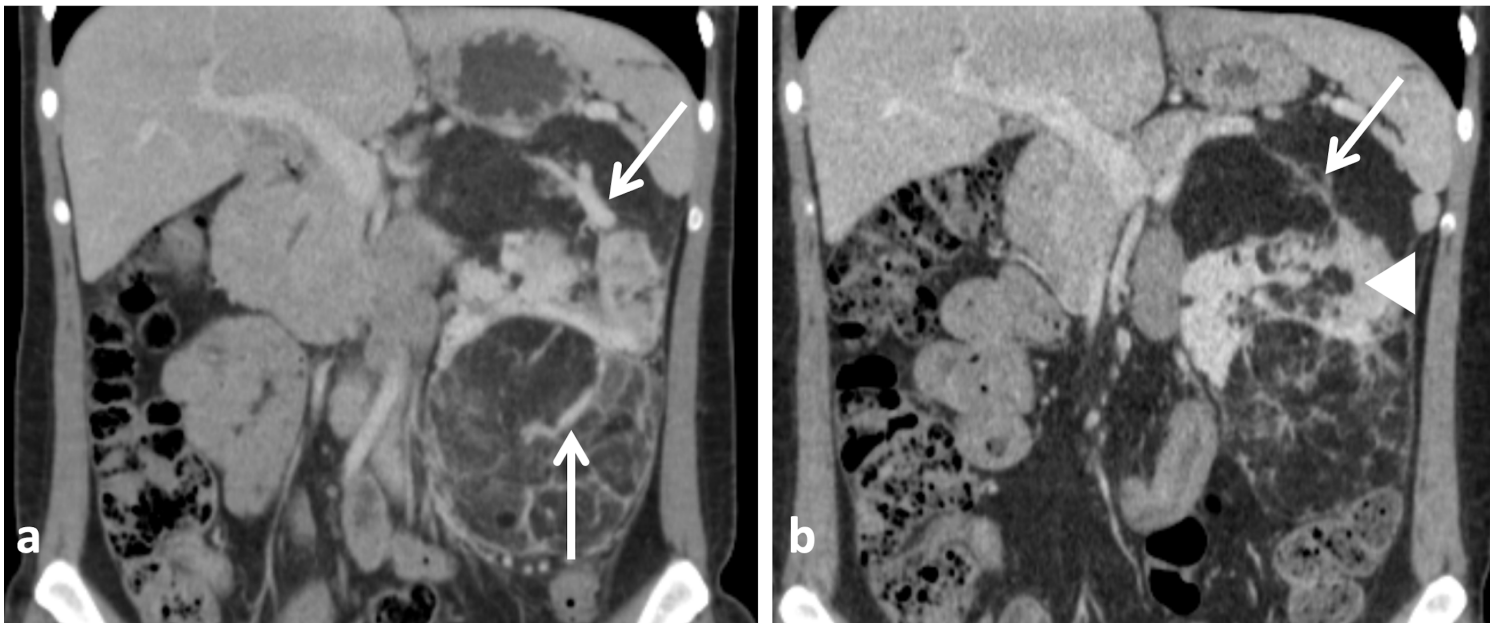

Figure 5

Response of intralesional vascular structures to sirolimus. Coronal nephrographic-phase CT images obtained (a) before the treatment and (b) after the treatment show disappearance of a left kidney large intralesional vascular structure and remarkable reduction of an intralesional aneurysm in response to treatment with sirolimus (arrows). An increase in the fat component is also seen (arrowhead).

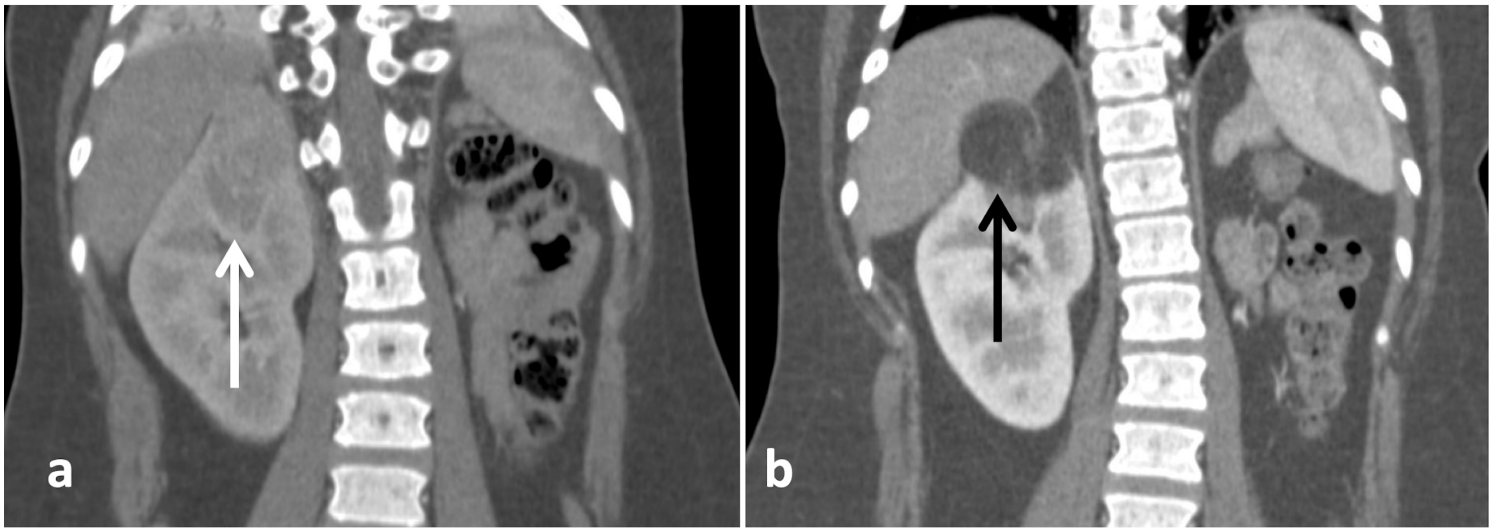

Figure 6

Liposubstitution in angiomyolipoma in response to treatment with sirolimus. Coronal corticomedullary-phase CT images obtained (a) before treatment and (b) after treatment show the effect of sirolimus treatment on a fat-poor AML in the upper pole of the right kidney (white arrow), revealing the appearance of a fat-rich tumor (black arrow) in substitution to the previous fat-poor pattern.

Supplementary Files

This is a list of supplementary files associated with this preprint. Click to download.

- FigureS1.SupplementaryFigure1.Histograms.tiff